LASER INTERFEROMETER GRAVITATIONAL WAVE OBSERVATORY

LIGO Laboratory / LIGO Scientific Collaboration

LIGO-T010145-00-D *ADVANCED LIGO* 11/20/01

LIGO Caltech 40-Meter PSL Commissioning Report

Dennis Ugolini, Peter King, Rich Abbott, Ben Abbott, Steve Vass, Alan Weinstein

Distribution of this document:
LIGO Science Collaboration

This is an internal working note
of the LIGO Project.

California Institute of Technology
LIGO Project – MS 18-34
1200 E. California Blvd.
Pasadena, CA 91125
Phone (626) 395-2129
Fax (626) 304-9834
E-mail: info@ligo.caltech.edu

Massachusetts Institute of Technology
LIGO Project – NW17-161
175 Albany St
Cambridge, MA 02139
Phone (617) 253-4824
Fax (617) 253-7014
E-mail: info@ligo.mit.edu

LIGO Hanford Observatory
P.O. Box 1970
Mail Stop S9-02
Richland, WA 99352
Phone 509-372-8106
Fax 509-372-8137

LIGO Livingston Observatory
P.O. Box 940
Livingston, LA 70754
Phone 225-686-3100
Fax 225-686-7189

http://www.ligo.caltech.edu/

Table of Contents

Table of Tables

Table of Figures

1 Introduction

The Caltech 40-meter prototype laboratory PSL was delivered and installed by Peter King and Lee Cardenas in May of 2001. It is essentially the same Nd:YAG Lightwave 1064 μm laser used at the main LIGO sites, except that the master oscillator is rated for 1 watt rather than 700 mW. The electronics were assembled and installed by Rick Karwoski, Paul Russell, and Sander Liu. At the time of this writing, the laser has been running for roughly 3000 hours. Measurements of the PSL performance over four months of commissioning at the 40-meter are presented in this document.

2 Optical Configuration

2.1 Table Layout

2.1.1 Initial Layout

Figure 1 shows a photograph of the current table layout for the 40-meter PSL, which is shown in more detail on the drawing in Figure 2. Note that our PSL table is 10x6 feet, different from those at the sites, and the layout has been adjusted accordingly.

A 70 mW beam is picked off of the main beam inside the laser casing and exits parallel to the main beam. Both beams pass through a pair of cylindrical lenses to correct astigmatism, and a periscope to bring the beam height down to three inches above the table. Pairs of mode-matching lenses are used to focus the beam into the major optical elements in each path.

The low-power beam (left half of Figure 2) is sent through a Pockels cell where 21.5 MHz sidebands are applied, then makes a double pass through an acousto-optic modulator (AOM) for a 160 MHz frequency shift. The beam then passes through another periscope and is locked to a suspended fixed-length reference cavity. The reflected light is read out by a tuned RF photodiode for use in frequency stabilization; the details of this feedback system are given in Chapter 3.

The main beam first passes through a half-wave plate/splitting cube combination, which allows us to attenuate the beam power to a desired level. Two steering mirrors then aim the beam into a pre-mode cleaner (PMC). Currently most of the transmitted light is send to a beam dump; roughly 1 mW is picked off and send to a pair of quad photodiodes to measure the position and angle of the beam leaving the PMC.

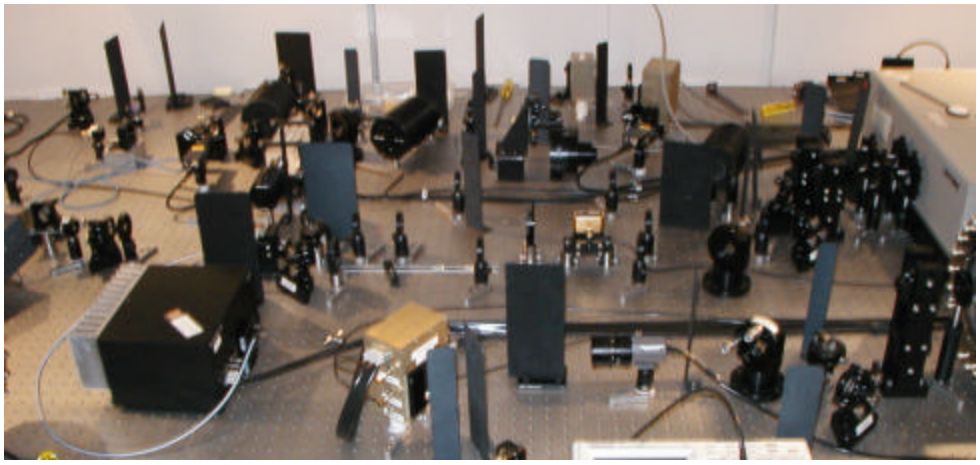

Figure 1: Photograph of 10'x6' PSL optical table

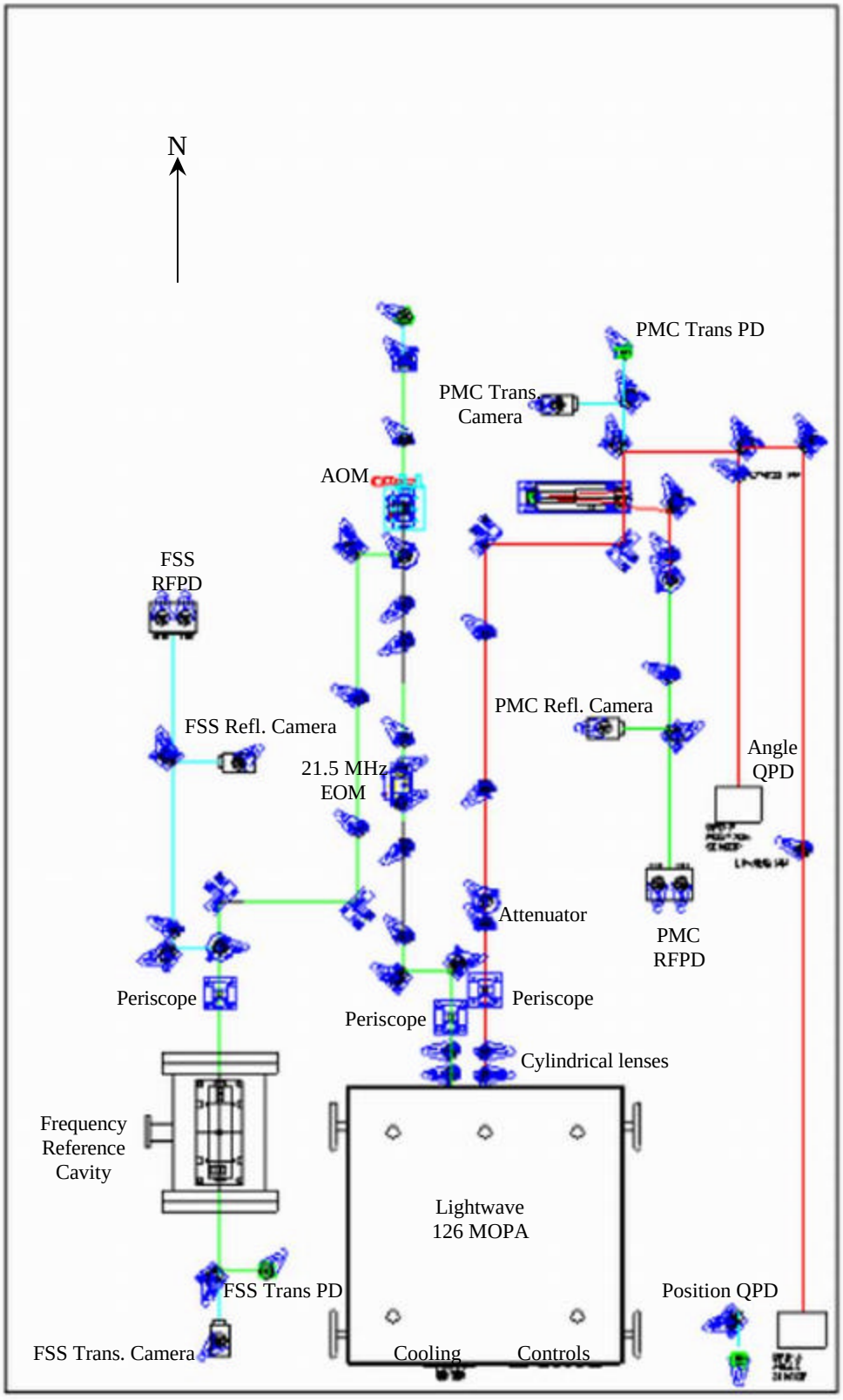

Figure 2: Initial layout of 40-meter PSL optical table

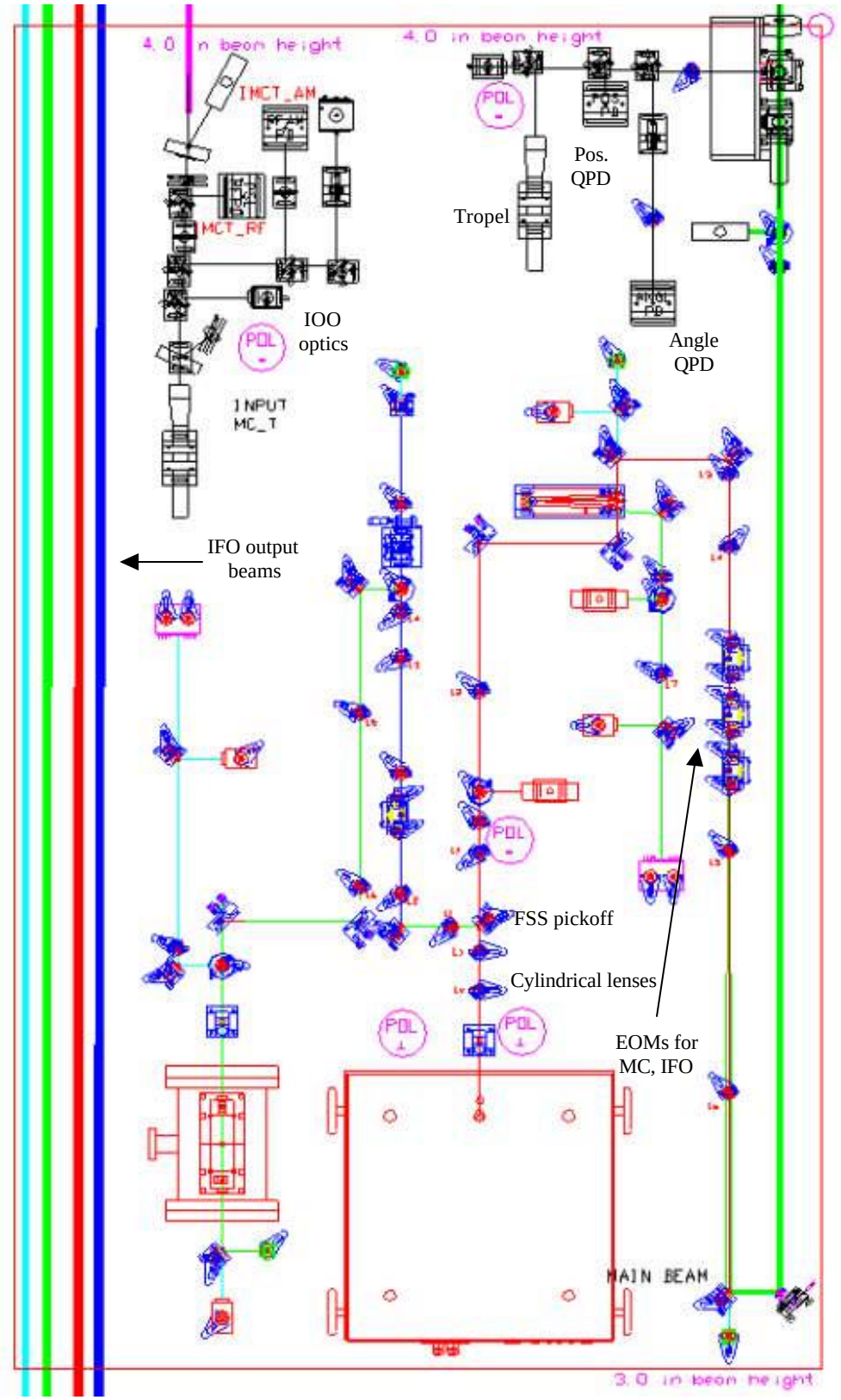

Figure 3: Proposed layout of 40-meter PSL optical table

2.1.2 Proposed Changes

Several changes in this layout are planned for the near future. Now that we have a better understanding of the beam width, the cylindrical and mode-matching lenses will be replaced and/or repositioned. Only one set of cylindrical lenses and one periscope will be used, with the low-power beam picked off after the periscope rather than inside the laser casing. The transmitted PMC path will be rearranged, with the high-power beam sent down and back the length of the table, mode-matched into three adjacent Pockels cells for adding the sidebands necessary for locking the IFO. At that time the QPDs will be moved to their permanent location on the northwest corner of the table, and anodized beam tubes will be inserted wherever the distance between optical elements is more than a couple of centimeters. This proposed final layout is drawn in Figure 3.

2.2 Beam Astigmatism

2.2.1 Initial Beam Parameters

The beam exiting the 126MOPA laser has horizontal and vertical beam waists that do not match in either width or position. These parameters were determined by picking off 1% of the main beam and measuring the horizontal and vertical beam width at many distances with a BeamScan device from Photon Inc. Fig. 4 shows the measured values along with a minimized chi-square fit, whose parameters are listed in Table 1.

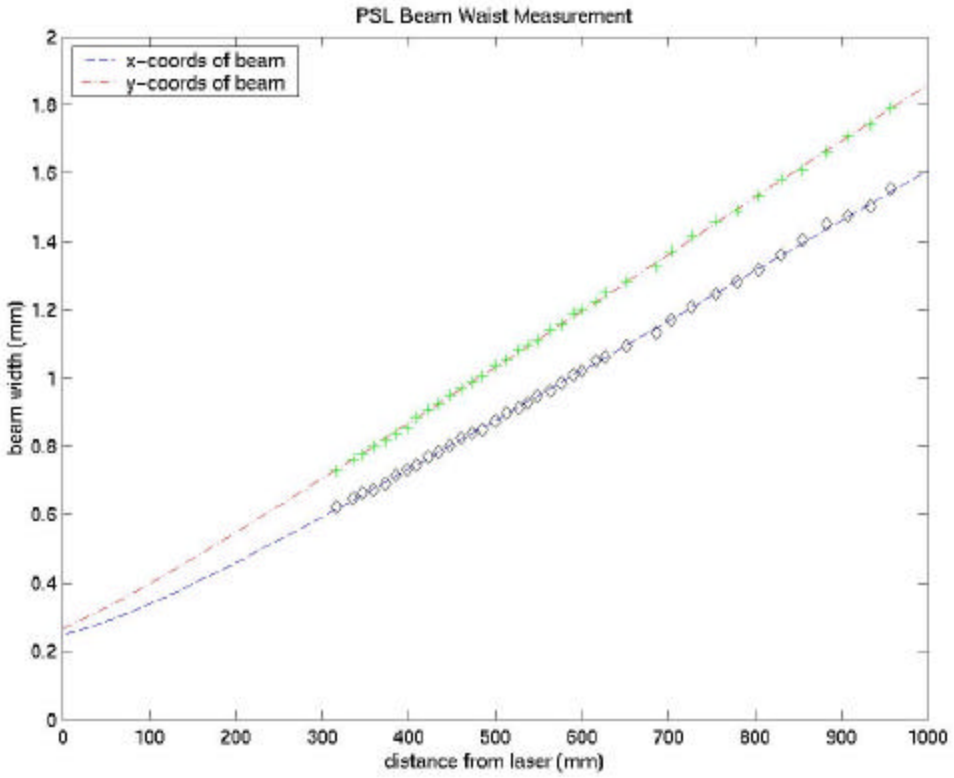

Figure 4: BeamScan measurements of beam width versus position

Table 1: Measurements of initial beam waist position and width

Beam Parameter	BeamScan measurement (11/01)	Installation measurement (5/01)
Horizontal width	0.227 mm	0.241 mm
Horizontal position	-67 mm	-164 mm
Vertical width	0.202 mm	0.166 mm
Vertical position	-103 mm	-182 mm

2.2.2 Cylindrical Lenses

Also shown in Table 1 are the beam parameters measured by Peter King when the laser was first installed. Based on these measurements, cylindrical lenses were chosen to correct the astigmatism: a vertical lens with f = 169.7 mm at z = 25 mm, and a horizontal lens with f = 282.0 at z = 85 mm. The model in Figure 5 shows that given the beam parameters measured recently, the cylindrical lenses do not correct the astigmatism. When the table layout is updated, we will replace these lenses with a horizontal lens with f = 565.5 mm at z = 328 mm and a vertical lens with f = 452.4 mm at z = 240 mm. The modeled improvement is shown in Figure 6.

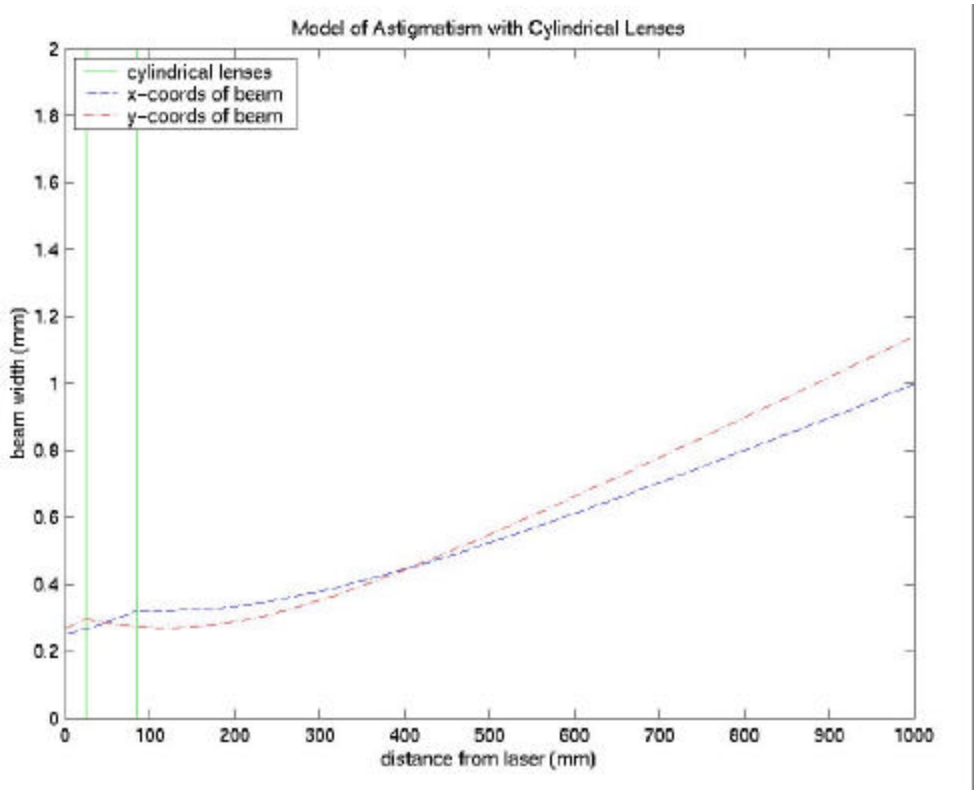

Figure 5: Model of beam astigmatism with current cylindrical lenses

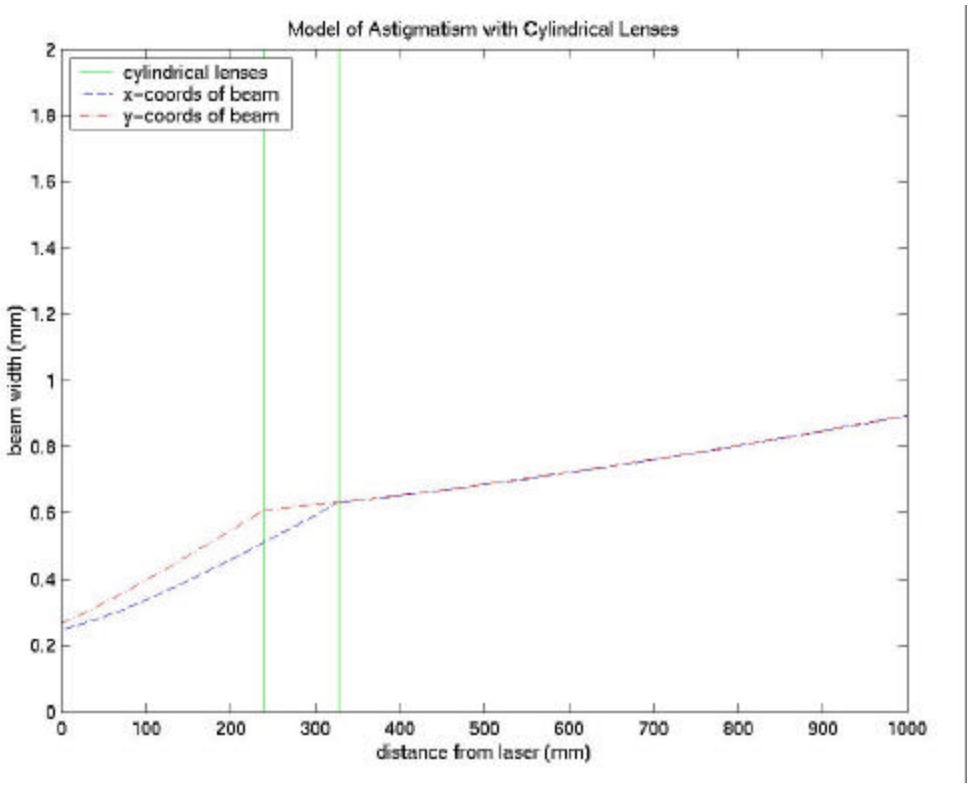

Figure 6: Model of proposed choice of cylindrical lenses

2.3 Mode Matching

The first column of Tables 2 and 3 give the mode matching lens focal lengths and positions for the pre-mode cleaner and reference cavity beam paths, respectively. Based on these lenses and the measured initial beam parameters, we constructed models of the beam width as a function of position for both paths, shown by the dashed curves in Figure 7. The vertical solid lines represent lenses (both mode-matching and cylindrical) as well as the spherical mirror at the AOM (roughly z = 1750 mm in the FSS path). The vertical dashed lines represent elements in the beam paths that should coincide with the beam waist, such as the EOM or the center of the reference cavity.

Table 2: Mode-matching schemes in PMC beam path

Optical element	Original layout		Proposed layout	
	Position (mm)	Focal length(mm)	Position (mm)	Focal length (mm)
cylindrical lens y	25	169.7	240	452.4
cylindrical lens x	85	282.0	328	565.5
lens	649	103.2	1256	160.4
lens	980	171.9	1568	160.4
EOM	1653.2	---	1662	---

Table 3: Mode-matching schemes in FSS beam path

Optical element	Original layout		Proposed layout	
	Position (mm)	Focal length(mm)	Position (mm)	Focal length (mm)
cylindrical lens y	25	169.7	240	452.4
cylindrical lens x	85	282.0	328	565.5
lens	483	103.2	448	114.5
lens	700	68.7	637	68.7
EOM	812.3	---	817	---
lens	1164	687.5	1174	286.5
lens	1247	286.5	1278	286.5
AOM	1429.7	---	1424	---
mirror (f = R/2)	1735	150.0	1724	150.0
AOM (return path)	2039.3	---	2024	---
lens	2562	1145.6	2496	572.7
lens	2846	687.5	2890	802.0
reference cavity	3867.5	---	3883	---

While close enough to allow good visibility in both cavities, there is room for considerable improvement in the mode-matching, especially at the AOM, where almost 75% of the light in the FSS path is lost due to the AOM's small aperture. The second column of Tables 2 and 3 gives an improved solution designed by Mike Smith, the results of which are modeled in Figure 8. The appropriate lenses will be installed when the table layout is updated in the near future. Note that the PMC model in Figure 8 includes the mode-matching into the EOMs past the PMC, which are necessary for locking the IFO but have not yet been installed.

3 Electronics Configuration

3.1 Rack Layout

Figure 9 shows the layout of the PSL electronics rack; a photograph of the completed rack is given in Figure 10. The rack was designed to resemble the PSL racks at the sites as much as possible, so that changes in wiring or layout could be more easily translated from one rack to another. Spare Sorenson power supplies have been included for future additions to the PSL or IOO electronics; the latter system inhabits the adjacent rack in the bay.

The PSL electronics are complete with two exceptions: the tidal compensation servo and the intensity stabilization servo. The HP 6267B power supply and Minco temperature controller for the tidal servo have been installed in the rack, and are ready for use when the frequency reference cavity heating jacket is delivered. The intensity stabilization servo board is not yet installed, but space has been reserved for it in the Eurocard crate.

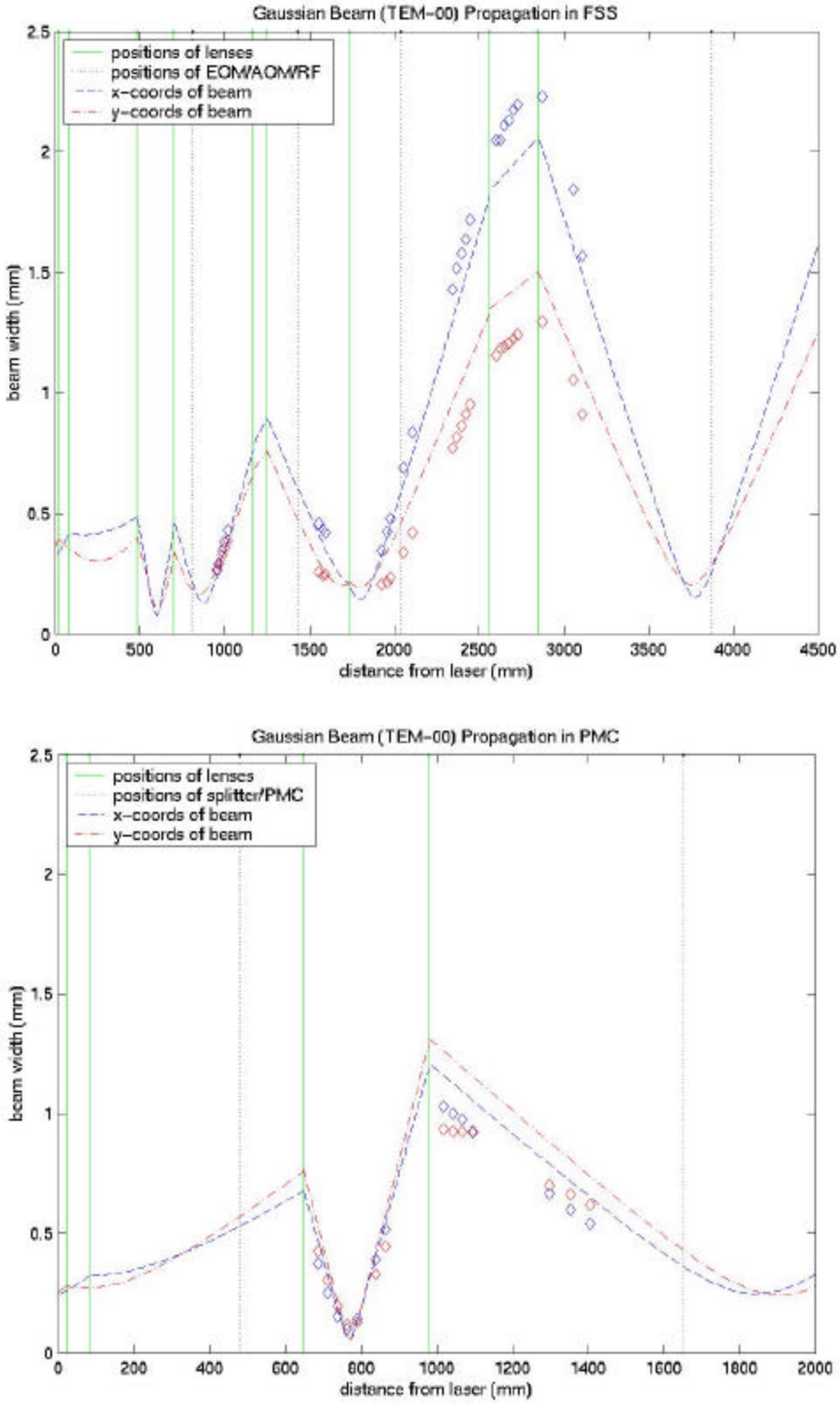

Figure 7: Model of mode-matching in FSS (top) and PMC (bottom) beam paths

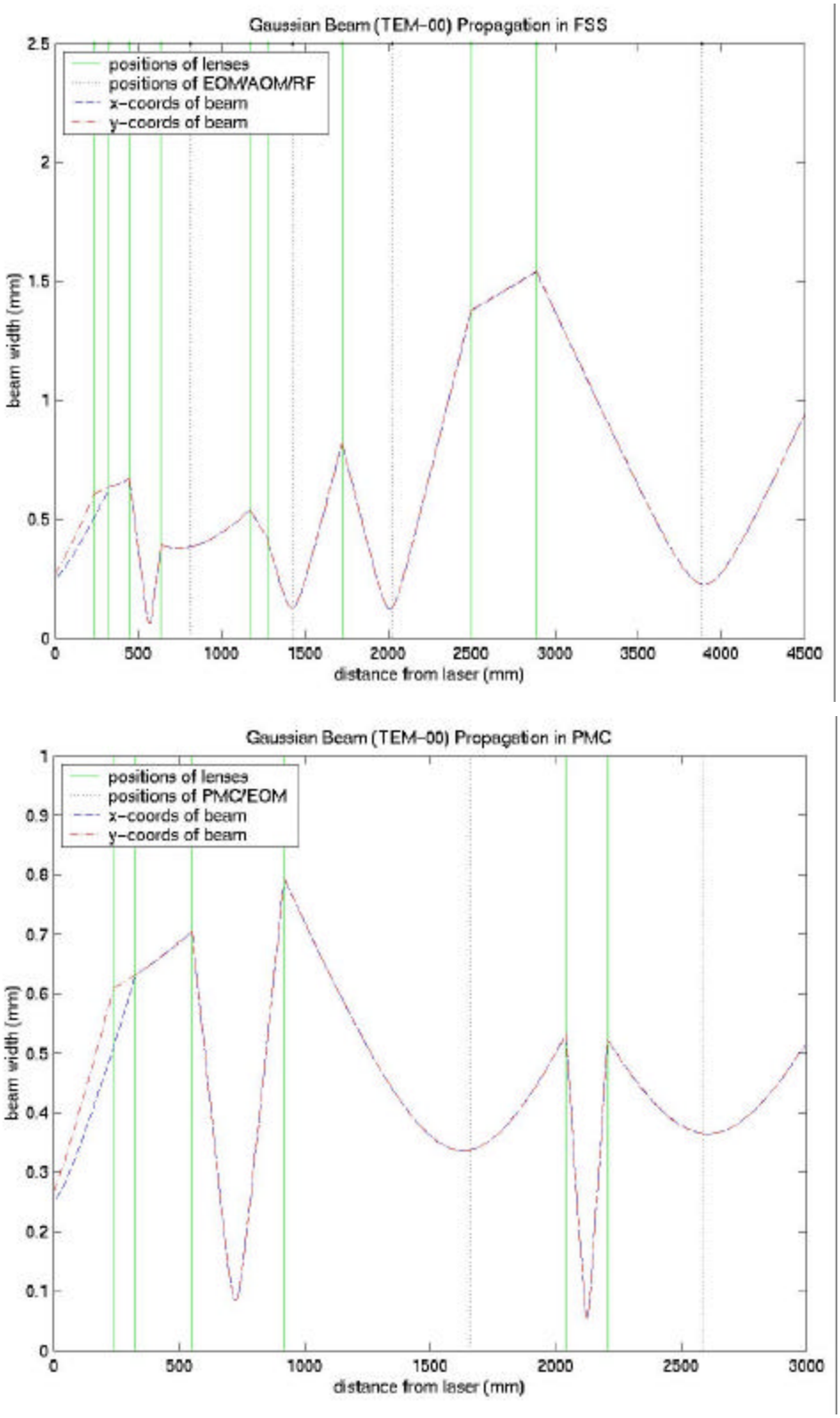

Figure 8: Model of proposed mode-matching solution in FSS (top) and PMC (bottom) beam paths

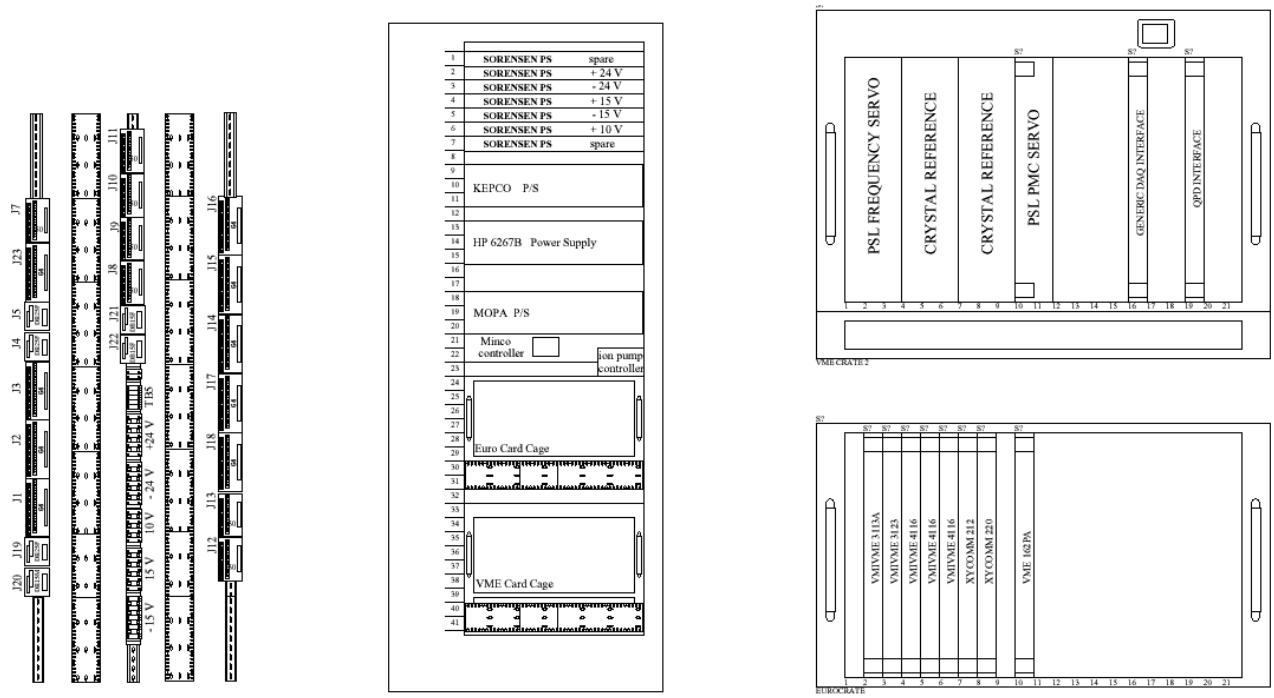

Figure 9: Layout of PSL rack electronics

Figure 10: Photograph of 40-meter PSL electronics rack

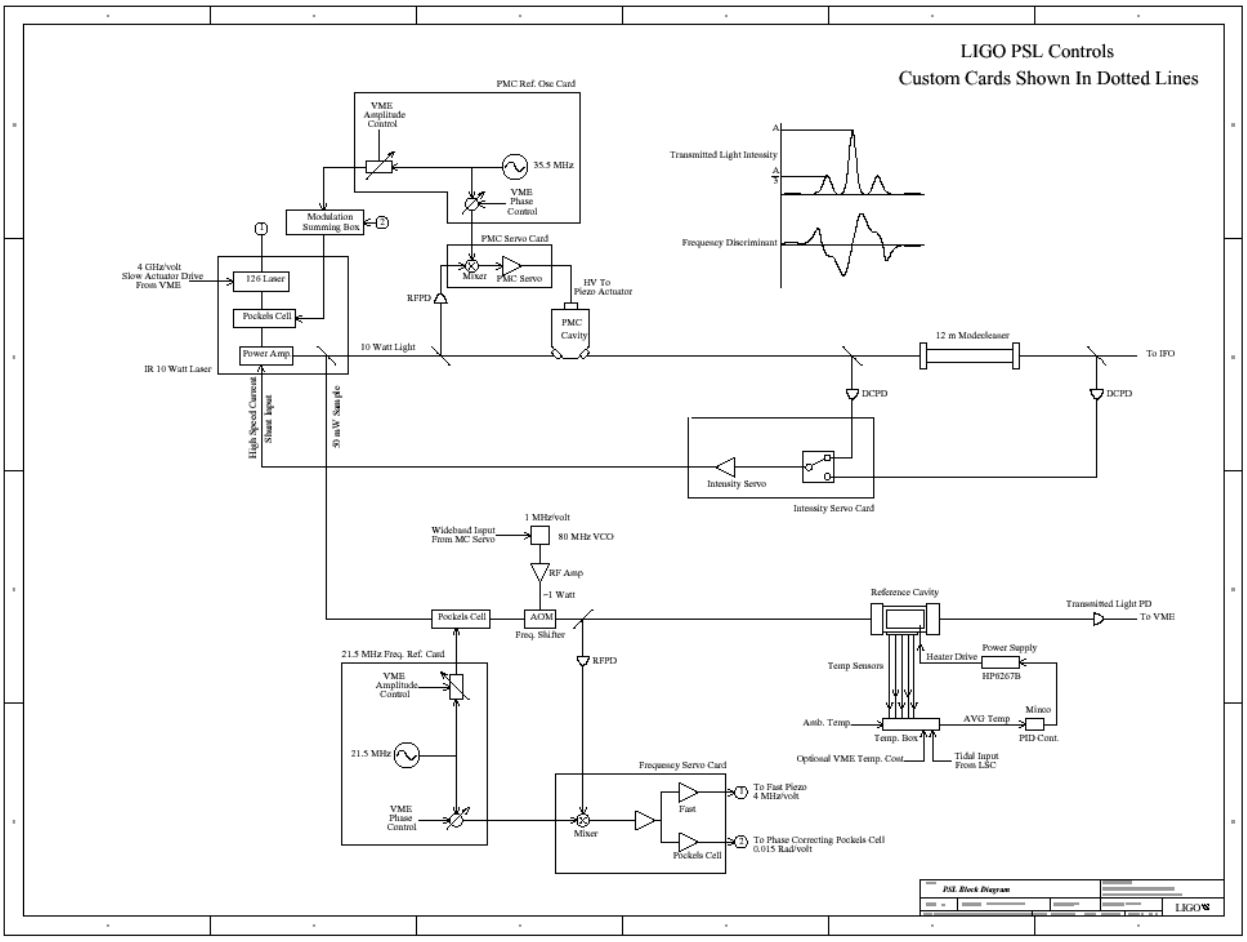

Figure 11: Conceptual block diagram of PSL controls

3.2 Servo Functionality

Figure 11 shows a conceptual block diagram of the PSL controls (LIGO document D000214-00-C). There are four main loops in the control system: the frequency stabilization servo (FSS), the pre-mode cleaner (PMC) locking servo, the intensity stabilization servo (ISS), and the tidal compensation servo.

Both the FSS and PMC servos mix modulated light with a frequency reference to generate an error signal for controlling one or more actuators. In the FSS, the modulation is supplied by a 21.5 MHz tuned Pockels cell in the low-power beam path (see Fig. 2). The error signal controls both a fast PZT actuator on the master oscillator and a phase-correcting Pockels cell inside the MOPA. There is also a slow software loop controlled by the VME processor, which adjusts a heater on the master oscillator based on the FSS error signal. The PMC modulation of 35.5 MHz is supplied by the phase-correcting Pockels cell, and the sole actuator is a PZT on the end mirror of the pre-mode cleaner cavity. Both of these servos are installed and working as intended.

The ISS will get light intensity information from two photodiodes, one measuring the PMC transmitted beam and the other measuring the 12m suspended mode-cleaner transmitted beam. A correction signal will be applied to a current shunt in the MOPA. The ISS is being developed by Rick Karwoski and Flavio Nocera and will be tested at the 40-meter.

The tidal compensation servo takes a control signal from the LSC electronics and applies it to a heating jacket wrapped around the frequency reference cavity vacuum chamber. While the 40-meter is too short to be sensitive to tidal forces, the servo also provides temperature stabilization for the laser, and furthers the goal of making the 40-meter as LIGO-like as possible. As previously mentioned, the power supply and temperature controller are in place, and the heating jacket should arrive before the end of November. The LSC system will be installed over the coming months.

3.3 DAQ Channels

The fast and slow DAQ channels reserved for the PSL are listed in Tables 4 and 5, respectively. The fast channels are sampled at 2 kHz, while the slow channels are pulled from the EPICS database at 16 Hz. An asterisk by a channel name in Table 5 indicates a user input from the EPICS screens.

4 Overall PSL Performance

4.1 Startup and Lock Acquisition

The laser must be running for roughly 20-30 minutes before it is "warmed up" enough for the servos to lock robustly. After this point, we have measured a typical startup time of about three minutes for an operator to lock both servos without the aid of automated acquisition software.

We have not measured the warmup time necessary for the PSL to reach its normal operating parameters. In general, we wait at least one day after laser startup before taking any important measurements.

4.2 Output Power

Figure 12 shows the output power of our laser from July 30th to November 27th of 2001, measured by a calibrated photodiode inside the laser casing. The gaps in the plot are due to shutdowns of both the PSL and the DAQ, which were commissioned at the same time. The output power is shown to have decreased from 10.7 watts to as low as 8.8 watts over the past four months.

Table 4: List of DAQ fast channels for PSL

Channel Name	Function
C1:PSL-FSS_MIXERM_F	FSS mixer output
C1:PSL-FSS_PCDRIVE_F	FSS control signal to phase-correcting Pockels cell
C1:PSL-FSS_SLOWDC_F	FSS control signal to master oscillator heater
C1:PSL-FSS_FAST_F	FSS control signal to fast PZT actuator
C1:PSL-ISS_ISERR_F	ISS error signal
C1:PSL-ISS_ISS_ACTM_F	ISS control signal to MOPA current shunt
C1:PSL-PMC_ERR_F	PMC error signal
C1:PSL-PMC_PZT_F	PMC control signal to end mirror PZT
C1:PSL-FSS_RFPDDC	Photodiode output for reference cavity reflected beam
C1:PSL-FSS_RCTRANSPD_F	Photodiode output for reference cavity transmitted beam
C1:PSL-PMC_RFPDDC_F	Photodiode output for PMC reflected beam
C1:PSL-PMC_TRANSPD_F	Photodiode output for PMC transmitted beam

Table 5: List of DAQ/EPICS slow channels for PSL

Channel Name (C1:PSL-)	Function		Channel Name (C1:PSL-)	Function
126MOPA_AMPMON	MOPA laser output power		FSS_VCODETPWR	VCO RF output monitor
126MOPA_126MON	Master oscillator output power		FSS_MIXERM	FSS mixer output
126MOPA_126PWR	Pump diode voltage		FSS_SLOWM	NPRO heater signal monitor
126MOPA_DTMP	Pump diode temperature		FSS_TIDALINPUT	not in use
126MOPA_LTMP	NPRO temperature		FSS_INOFFSET*	FSS loop input offset
126MOPA_DMON	Pump diode output power		FSS_MGAIN*	FSS loop common gain
126MOPA_LMON	NPRO output power		FSS_FASTGAIN*	FSS loop fast gain
126MOPA_CURMON	Pump diode current		FSS_PHCON*	21.5 MHz phase adjust
126MOPA_DTEC	Pump diode TEC		FSS_RFADJ*	21.5 MHz mod. depth adjust
126MOPA_LTEC	NPRO TEC		FSS_SLOWDC*	Control signal to NPRO heater
126MOPA_CURMON2	Power amplifier diode current		FSS_VCOMODLEVEL*	VCO modulation depth adjust
126MOPA_HTEMP	Power amplifier temperature		FSS_TIDALSET	not in use
126MOPA_HTEMPSET	Power amp temp. setpoint		ISS_AOMRF	not in use
126MOPA_126CURADJ	not in use		ISS_ISERR	ISS error signal – not in use
126MOPA_DCAMP	not in use		ISS_GAIN	ISS loop gain – not in use
126MOPA_PZT+	not in use		ISS_ISET	not in use
126MOPA_PZT-	not in use		PMC_PMCTLL	not in use
FSS_RFPDDC	Photodiode: FSS reflected		PMC_RFPDDC	Photodiode: PMC reflected
FSS_LODET	Local osc. signal amplitude		PMC_LODET	Local osc. signal amplitude
FSS_FAST	Control signal to fast PZT		PMC_PMCTRANSPD	Photodiode: PMC transmitted
FSS_PCDRIVE	Signal to phase-corr. EOM		PMC_PZT	Signal to end mirror PZT
FSS_RCTRANSPD	Photodiode: FSS transmitted		PMC_MODET*	35.5 MHz modulation depth
FSS_RCTLL	not in use		PMC_PMCERR	PMC servo error signal
FSS_TIDALOUT	not in use		PMC_GAIN*	PMC servo loop gain
FSS_MODET*	21.5 MHz modulation depth		PMC_INOFFSET*	PMC servo loop input offset
FSS_MINCOMEAS	not in use		PMC_PHCON*	35.5 MHz phase adjust
FSS_RMTEMP	not in use		PMC_RFADJ*	35.5 MHz mod. depth adjust
FSS_RCTEMP	not in use		PMC_RAMP*	PZT DC output adjust

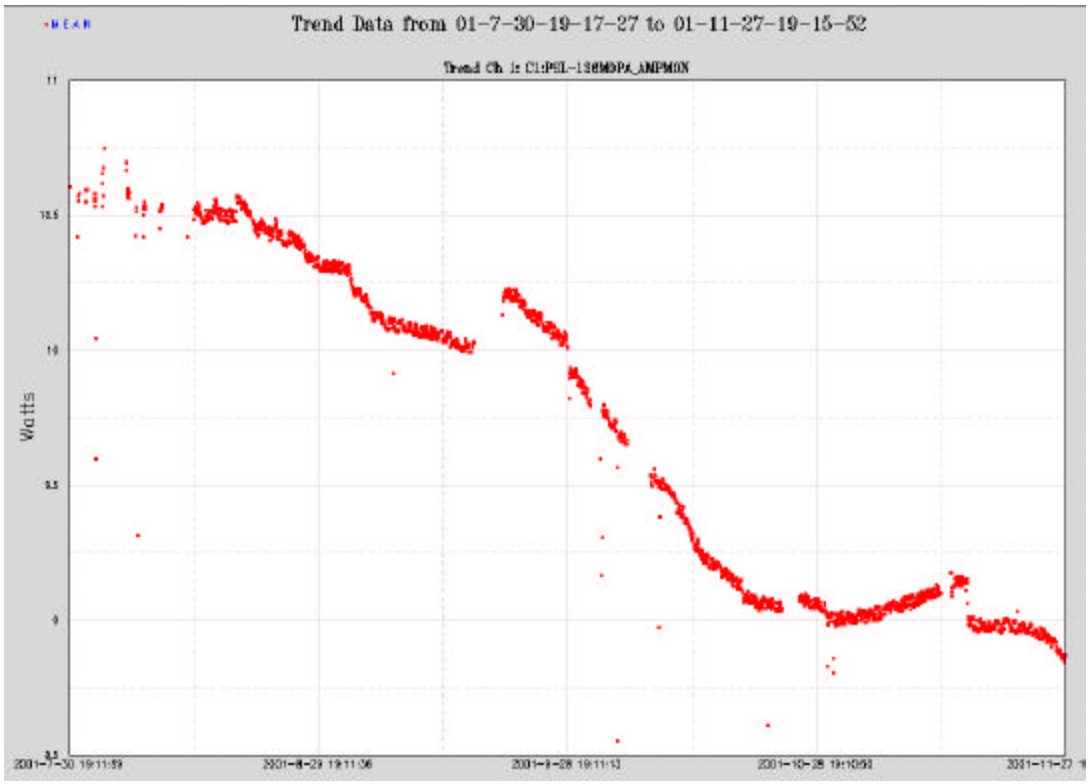

Figure 12: PSL output power from July-November, 2001

The PSL design requirement for power transmission in the main beam path (through the pre-mode cleaner) is 8.5 watts, as stated in the LIGO PSL Conceptual Design Report (T970087-04-D). The highest measured power transmission at the 40-meter is 6.1 watts, with an incident beam intensity of 8.7 watts (measured by calorimeter). The low power output is believed to be due to a PMC curved mirror with a larger transmission than desired. This mirror will be replaced in the near future.

4.3 Chilled Water Cooling

The one-watt master oscillator requires a constant supply of chilled water to remain at an operating temperature of 22.0 degrees Celsius. There is a needle valve in the laser casing that controls the flow rate of chilled water to the master oscillator. We have found that if this valve is not kept wide open, the laser temperature will quickly rise above 30 degrees Celsius and the power supply will shut down. This is contrary to the sites where, presumably because the oscillator runs at a lower power, the flow rate is much lower; we have been told that LHO can run with no cooling at all.

We also found a water leak where the chilled water first enters the laser casing. The water enters a small plastic box with two screw-in plugs, each of which had only a single turn of Teflon tape around the threads, allowing a significant amount of water to spill onto the floor of the laser casing. We rewound the plugs with eight layers of Teflon tape, and the leak has not reoccurred.

4.4 TEM_{00} Transmission

Figure 13 shows the BeamScan measurement of the PMC transmitted beam, with the horizontal and vertical cross-sections fit with a Gaussian (blue). The excellent fit proves that the transmitted beam is TEM_{00} mode to a high degree.

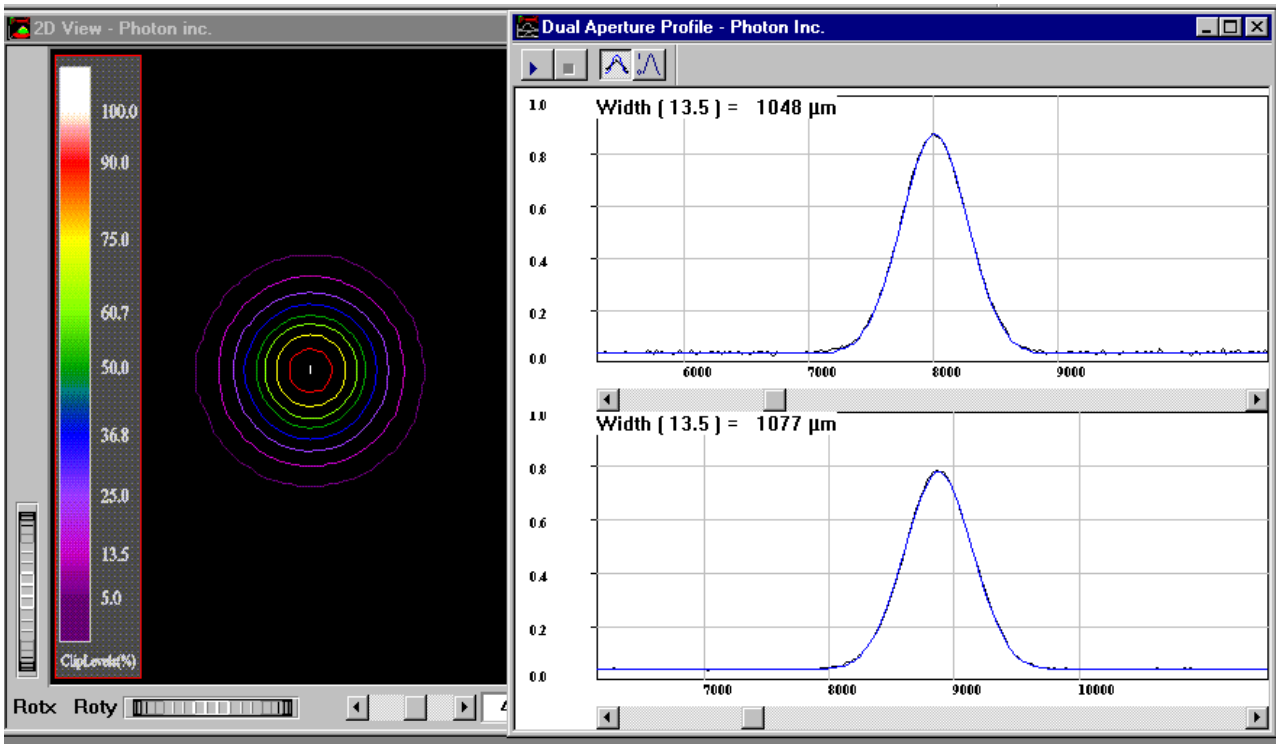

Figure 13: Measured cross-section of PMC transmitted beam

4.5 Locking Stability

Though we have been frequently breaking lock during the commissioning process, our trend frame data suggests that the PSL remains locked and functional throughout a typical weekend.

4.6 Position/Angle Stability

We have used quad photodiodes (QPDs) to determine the low and high-frequency stability of the PMC transmitted beam in position and angle. For low-frequencies, we read the QPDs into frame data over a period of 60 hours, with the results shown in Figure 14. Some temperature dependence can be seen, particularly in position. The QPDs were calibrated by shifting them on an x-y micrometer stage and monitoring their readout; the position calibration was also verified by inserting microscope slides of various thicknesses at a 45^0 angle and measuring the displacement. A change of one volt in the QPD readout corresponds to a translation of 60 µm in position or rotation of 65 µrad in angle of the PMC transmitted beam. As can be seen in Figure 14, the drift in position over the 60-hour period was 27 µm horizontally and 25 µm vertically. Since the beam is focused to a radius of 0.36 mm at the EOMs downstream of the PMC, the drift is no more than 8% of the width of the beam. In angle, the long-term drift equaled 18 µrad horizontally and 20 µrad vertically. The divergence angle of the beam is $\lambda/\pi\omega_0$ = 940 µrad; the drift in angle does not exceed 3% of this quantity.

The high-frequency behavior for position and angle are given in Figures 15 and 16, respectively. The periodic shape of the spectra is poorly understood, but is probably due to how the spectrum analyzer samples each decade of frequency, revealed here because the signal is close to the analyzer's noise floor. The origin of the peaks at 700 Hz and 22 kHz is not known. The noise is below 0.04 µm rms in position and 0.4 µrad rms in angle, more than an order of magnitude smaller than the low-frequency drift.

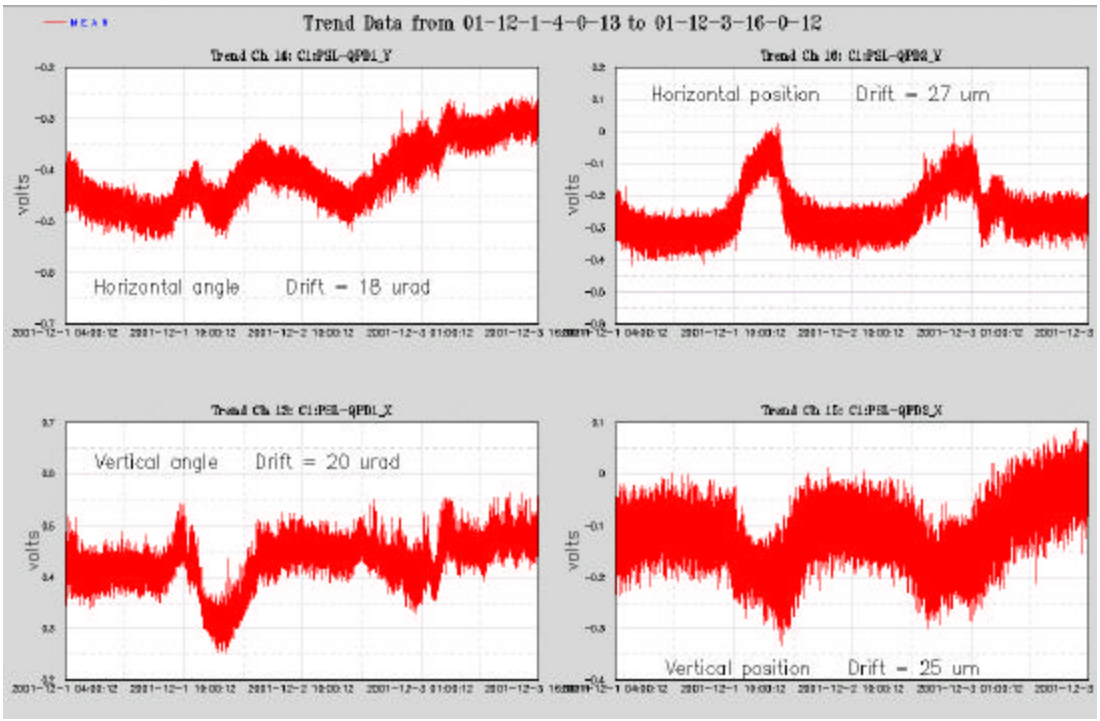

Figure 14: Placeholder for 60-hour beam drift plot

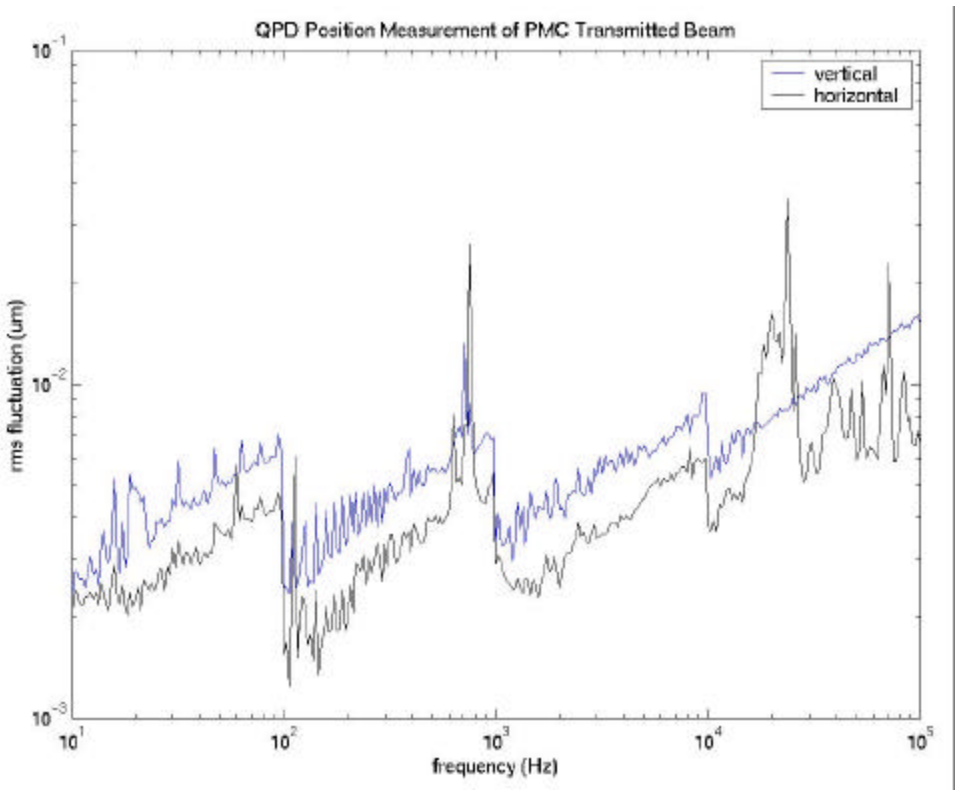

Figure 15: QPD measurement of high-frequency beam position jitter

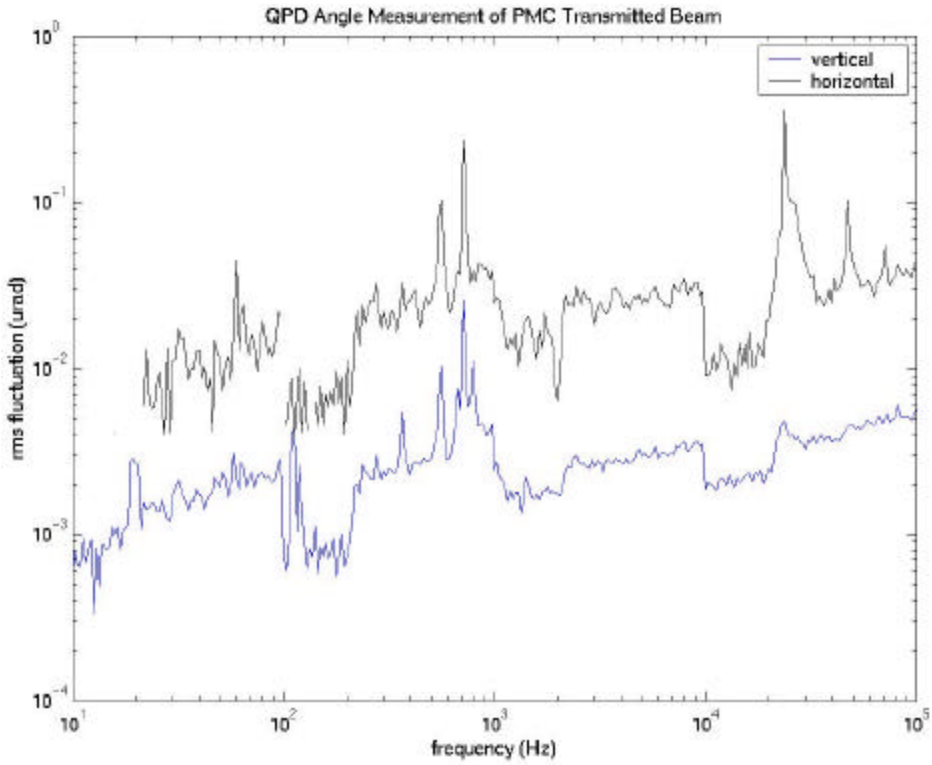

Figure 16: QPD measurement of high-frequency beam angle jitter

4.7 Intensity Stability

There is currently no intensity stabilization servo installed in the 40-meter PSL. Figures 17 shows the high-frequency behavior of the reflected and transmitted beams from the reference cavity and PMC, expressed as a fraction of the total light intensity at each photodiode. The periodic structure of the plots is again probably an artifact of signals near the noise floor of the spectrum analyzer. There are no outstanding features other than a small peak at 730 Hz in the PMC transmitted beam whose source is not known. Despite the poorly-understood structure of the spectrum analyzer output, we can see no noise sources that rise above 0.2% of the total beam intensity.

5 Frequency Stabilization Servo (FSS) Performance

5.1 Cavity Parameters

The frequency reference cavity is a suspended 20.3 cm tube with fixed mirrors at either end, and a finesse of roughly 9500. Figure 18 shows a Matlab model of the transmission, reflection, and error signal expected as a function of frequency.

We can reveal this error signal in the FSS mixer output on an oscilloscope by ramping the fast PZT actuator through resonance with the loop closed. We do this by first locking the FSS servo to resonance, and then inserting a 10 Hz, 10 V sawtooth wave at the Ramp Input connection on the servo board. The resulting scope trace is shown in Figure 19. A distorted error signal for this servo loop had been shown at the 40m Conceptual Design Review (G010385-00-R); this was found to be caused by a broken connection in the RF photodiode.

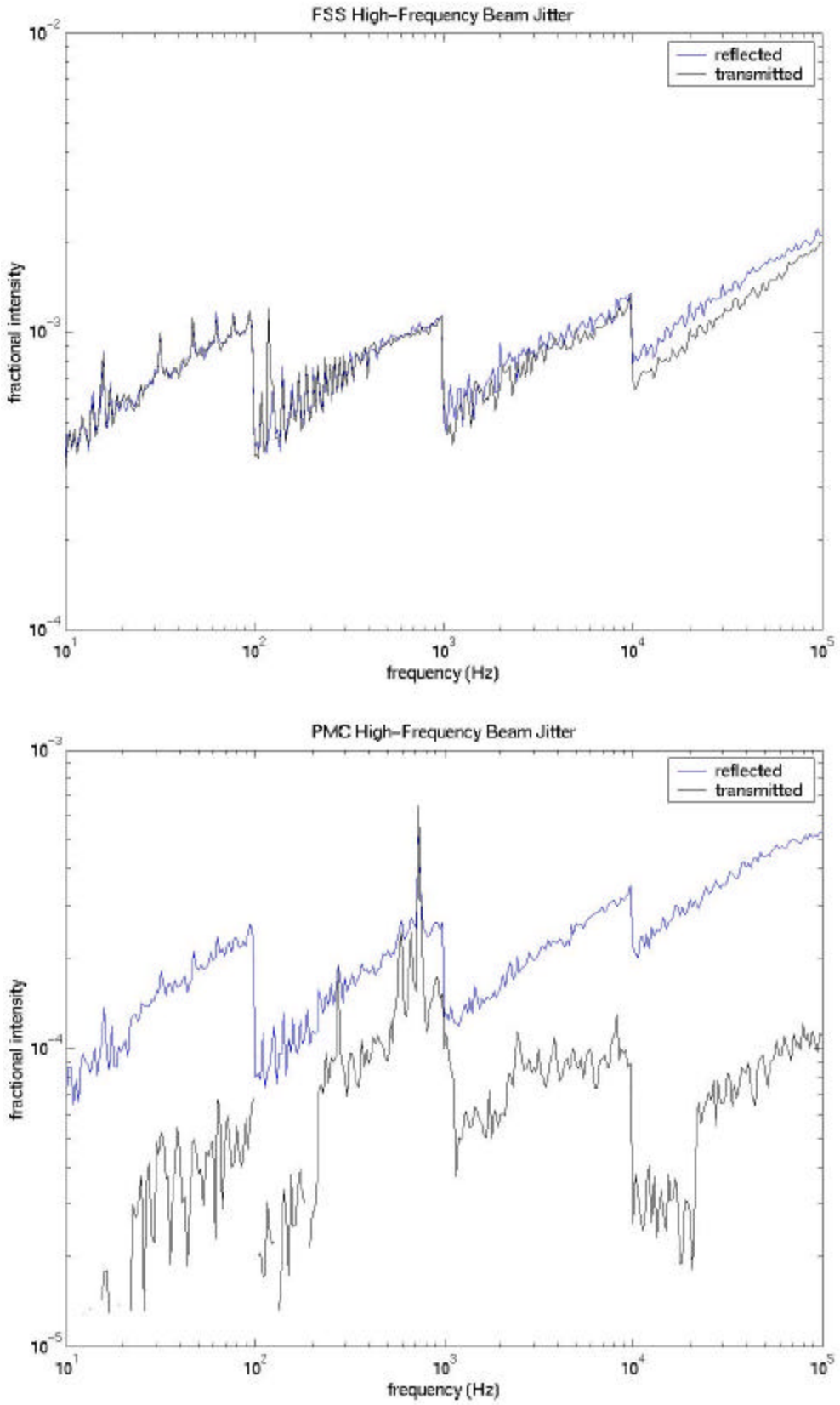

Figure 17: High-frequency behavior of FSS (top) and PMC (bottom) beams

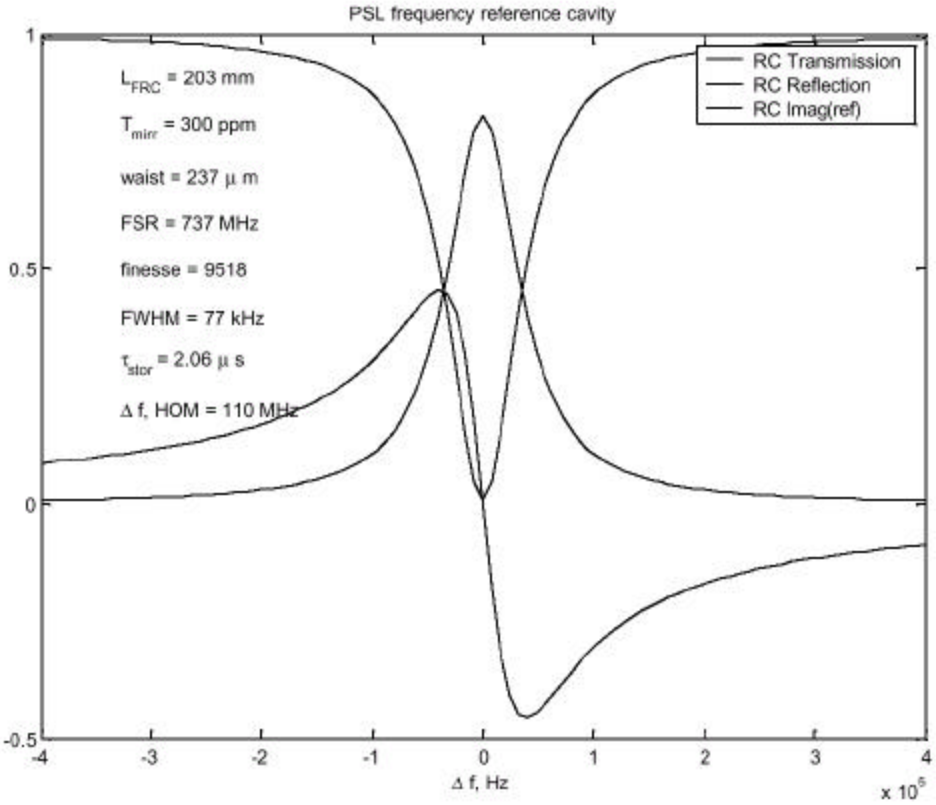

Figure 18: Model of reference cavity reflection, transmission, and error signal

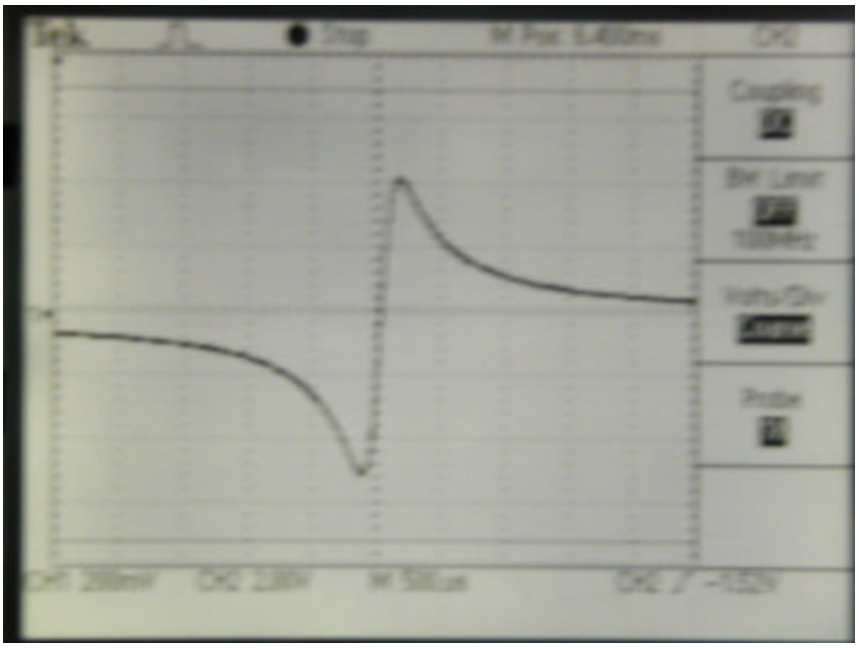

Figure 19: Oscilloscope trace of FSS servo error signal

5.2 Cavity Visibility

Cavity visibility is measured by ramping the servo through resonance in the same manner as for the error signal measurement, and viewing the DC output of the RFPD. The visibility is given by $(1-V_{on})/V_{off}$, where V_{on} and V_{off} are the voltage outputs of the RF photodiode on and off resonance. Note that the RF modulation must be shut off, since power in the sidebands will be reflected on and off resonance, leading to an incorrect ratio. Figure 20 shows a photograph of the oscilloscope trace during such a measurement. The fixed reference cavity visibility has been measured to be 93%, with ~5 mW of transmitted power. The low power output is due to losses at the AOM, which are in turn due to mode mismatch.

5.3 Servo Transfer Function

The LIGO PSL CDS Conceptual Design Report (970114-00-D) lists the design requirements for the FSS and PMC servos, including the unity gain frequencies and in-loop frequency noise limits. The requirement for the FSS transfer function is a unity gain frequency of 500-800 kHz.

The transfer function is measured by sending a 50 mV sine wave from the spectrum analyzer to Test Input 2 on the FSS servo board, and sweeping from 100 Hz to 100 kHz while the servo is locked. There is a single op-amp between this input and the mixer monitor output on the servo board. The ratio of output to input is equal to the expression G/(1+GH), where H is the transfer function we are looking for and G is the gain of the op-amp, measured by repeating the measurement with the loop open. Figure 21 shows this measured transfer function; extrapolating to higher frequencies gives a unity gain frequency of roughly 220 kHz. The irregular shape of the curve is not "real" structure, but a reflection of noise in the mixer output of similar amplitude to the injected signal, which is in turn a sign that the gain in the loop is too small.

The spectrum in Figure 21 was measured with the FSS Common Gain set to +20 dB and the FSS Fast Gain at the maximum of +30 dB, to compensate for the small error signal from the servo board mixer. There are two reasons for the small error signal: a smaller-than-expected signal from the local oscillator board, and very little light reaching the RFPD. The former problem was solved by changing the resistor values of a 50-ohm "T" attenuator on the local oscillator board, boosting the signal by a factor of three (the measurement in Figure 21 was taken after this fix). The small RFPD signal should be fixed once the new mode-matching solution is installed, reducing the losses at the AOM. At that point we may have enough gain in the loop to reach the unity gain design requirement and eliminate the noise in the transfer function measurement.

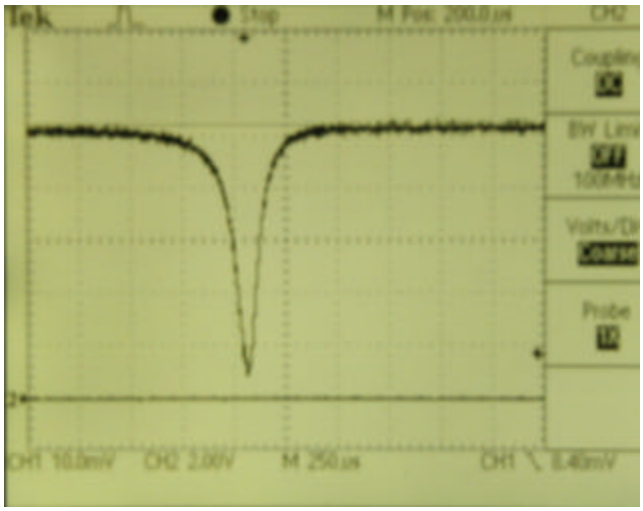

Figure 20: Oscilloscope trace of reference cavity visibility measurement

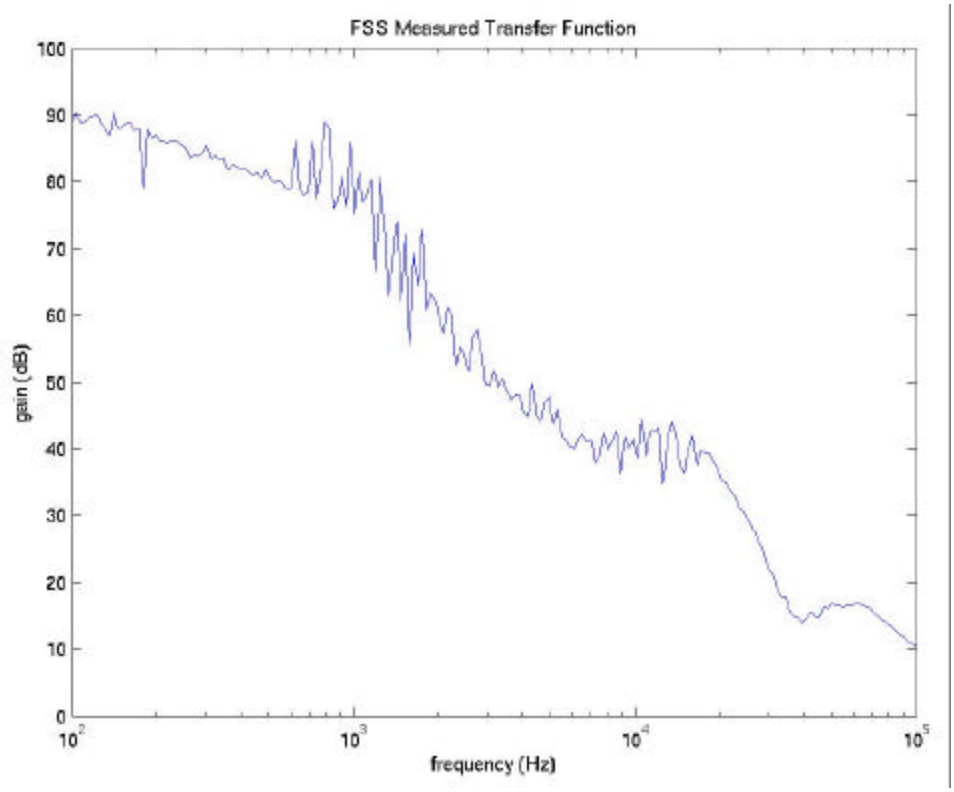

Figure 21: Measured transfer function of FSS servo loop

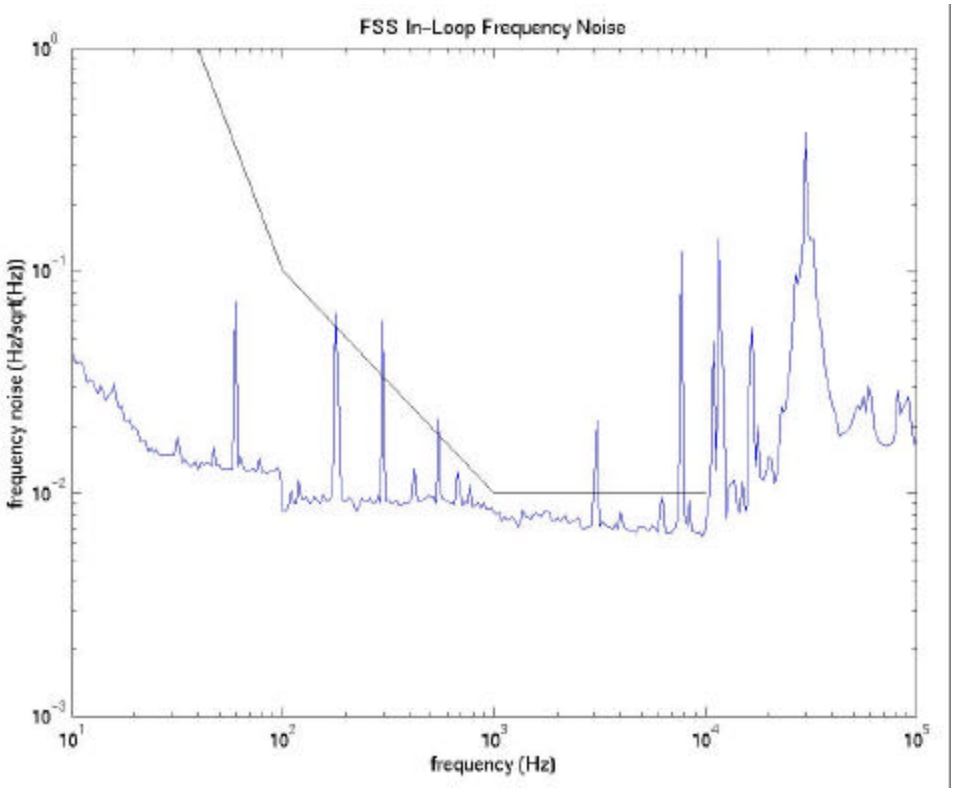

Figure 22: Measured FSS in-loop frequency noise versus design requirement

5.4 In-loop Frequency Noise

The design requirement for the FSS in-loop frequency noise is a limit of 0.1 Hz/√Hz at 100 Hz, descending to a limit of 0.01 Hz at 1 kHz and above. This limit is shown by the solid black curve in Figure 22, along with the measured noise. With the exception of 60 Hz harmonics, our FSS meets the design requirement.

6 Pre-Mode Cleaner Servo (PMC) Performance

6.1 Cavity Parameters

The pre-mode cleaner cavity is an isosceles triangle of mirrors (3 cm base, 19 cm height) on a fixed glass block, with a finesse of roughly 4000. The mirrors at the base of the triangle are fixed, while the high-reflectance end mirror is controlled through a PZT actuator by the PMC servo loop to maintain resonance. Figure 23 shows a Matlab model of the transmission, reflection, and error signal expected as a function of frequency. The measured error signal, shown in Figure 24, is generated by injecting a 10 Hz, 2 V sawtooth wave in the EXT DC input on the PMC servo board while the cavity is locked at resonance.

6.2 Cavity Visibility

The pre-mode cleaner visibility has been measured to be 83%, with 6.1 W of transmitted power. As previously mentioned, the PMC end mirror has a higher transmission than expected. Replacing this mirror should improve the power output, and improving the mode-matching may bring the cavity visibility in line with that of the reference cavity.

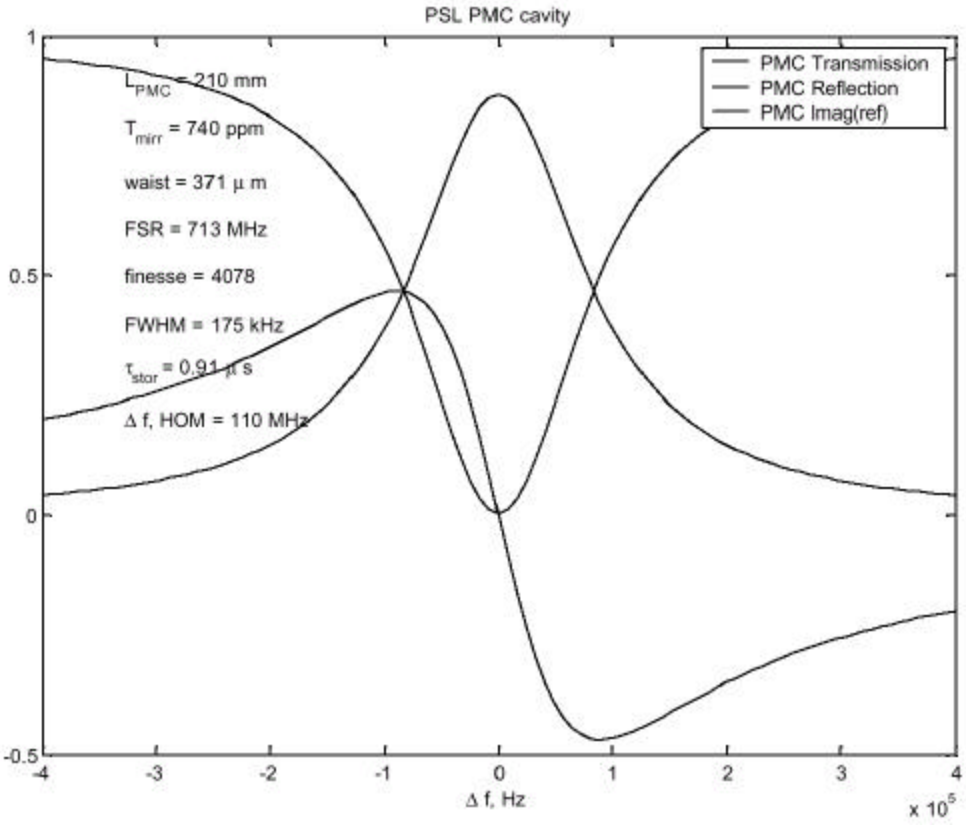

Figure 23: Model of PMC reflection, transmission, and error signal

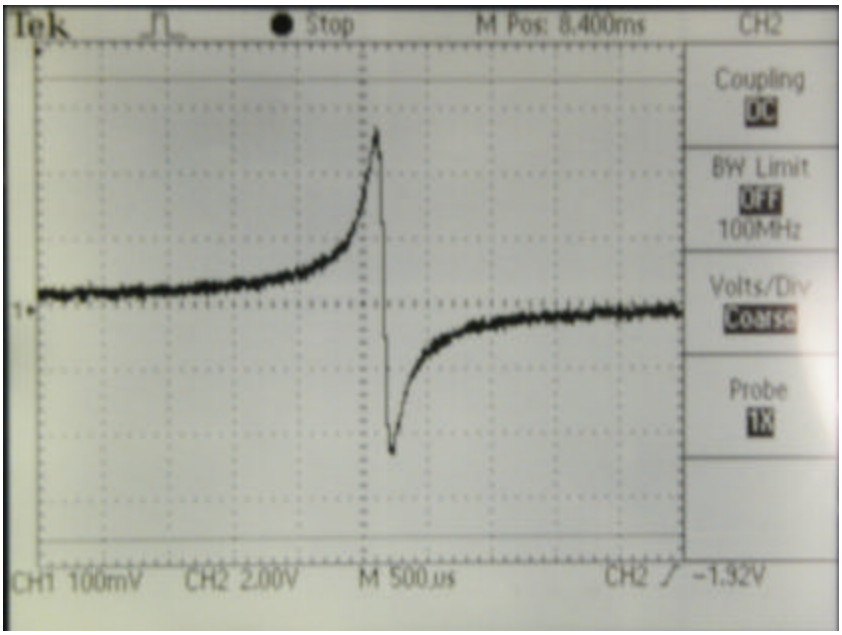

Figure 24: Oscilloscope trace of PMC servo error signal

6.3 Servo Transfer Function

The design requirement for the PMC transfer function is a unity gain frequency of no less than 600 Hz. The transfer function is measured in the same way as for the FSS servo (see section 4.2); the results are shown in Figure 14. The unity gain frequency is 1.58 kHz, well above the design requirement.

When first commissioning the PMC servo, we discovered a large resonance at 31.3 kHz, so large that the servo could only be locked if the loop gain was reduced to a minimum and the light to the RFPD greatly attenuated. We do not know the source of this resonance, but Ben Abbott added a notch filter at the output to the PZT actuator on the PMC end mirror to cancel the effects of the resonance. The large dip at 30 kHz in the transfer function corresponds to this filter.

The PZT actuator has a known resonance of roughly 65 kHz, which is identified in Figure 14. The source of the higher frequency peak is unknown.

6.4 In-loop Frequency Noise

The frequency noise requirements of the PMC servo are much less stringent than those of the FSS servo; the noise limit falls from 165 to 1.65 Hz/$\sqrt{}$Hz over a frequency range of 100 Hz to 10 kHz. Figure 15 shows the in-loop frequency noise versus this limit, measured with the frequency stabilization loop open.

7 Summary and Acknowledgements

The 40-meter PSL is locking robustly and meeting the design requirements for the FSS and PMC servos. New mode-matching and cylindrical lenses have been ordered, and once installed, the cavity visibilities and power transmission should meet expectation. At this point the PSL will be ready for the arrival of the 12m suspended mode cleaner optics in mid-February, and will also serve as the intensity stabilization servo testbed as needed.

The authors would like to thank Lee Cardenas, Rick Karwoski, Paul Russell, Sander Liu, Rick Savage, Tim Piatenko, and Andrea deMichele for their time and assistance throughout the commissioning process.

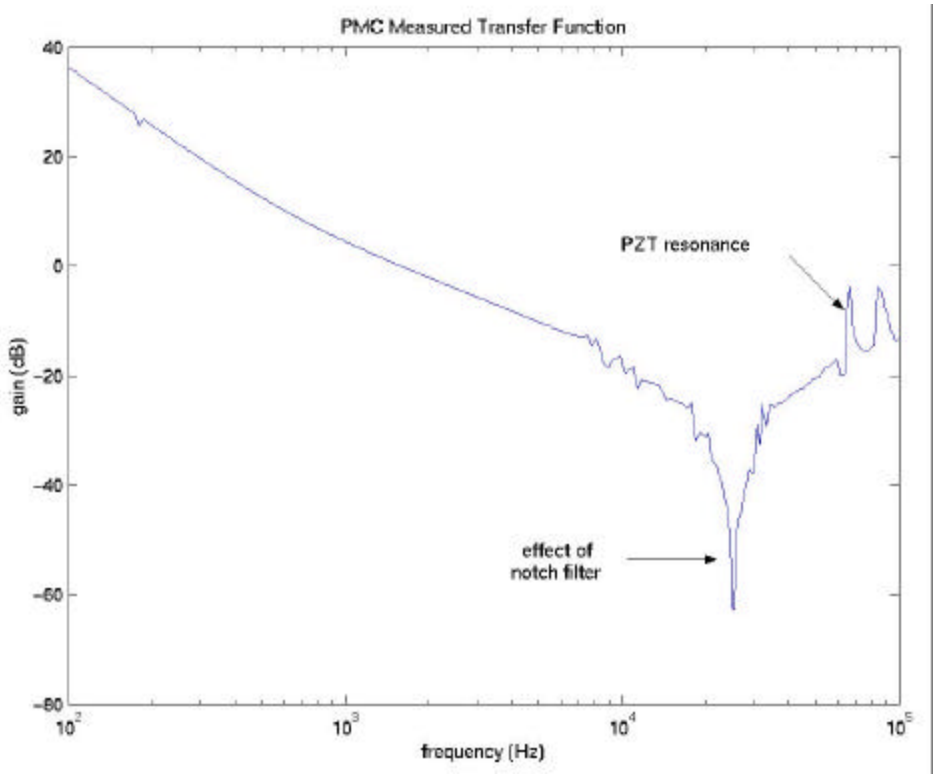

Figure 25: Measured transfer function of PMC servo loop

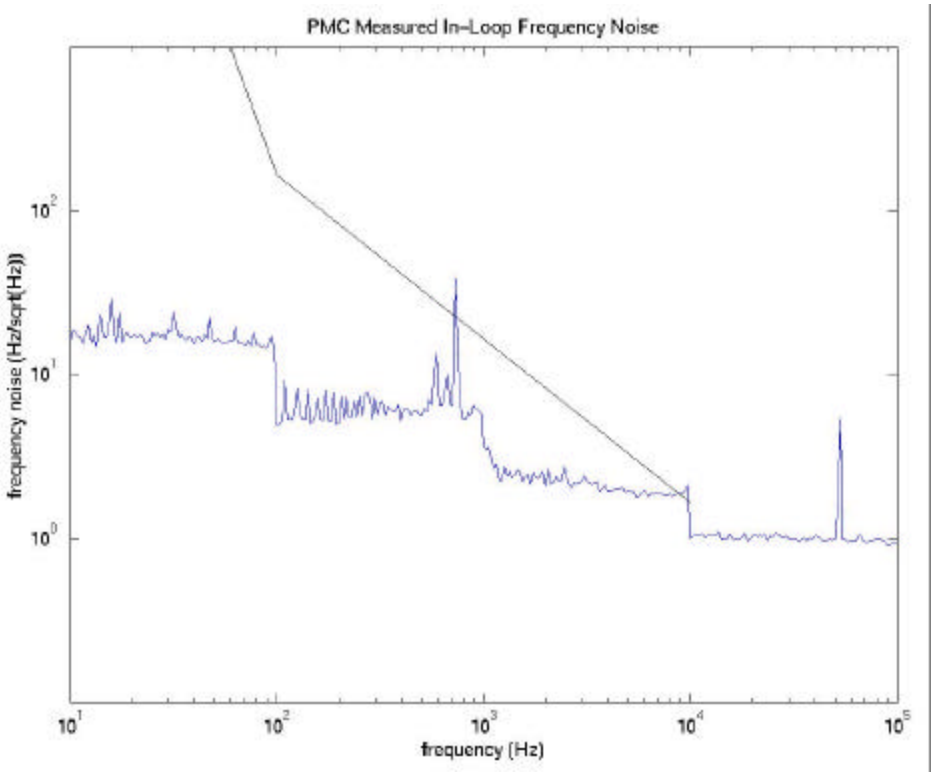

Figure 26: Measured in-loop frequency noise of PMC servo versus design requirement